

Chemical Science

Accepted Manuscript

This article can be cited before page numbers have been issued, to do this please use: U. Dutta, G. Prakash, K. Devi, K. Borah, X. Zhang and D. Maiti, *Chem. Sci.*, 2023, DOI: 10.1039/D3SC03528J.



This is an Accepted Manuscript, which has been through the Royal Society of Chemistry peer review process and has been accepted for publication.

Accepted Manuscripts are published online shortly after acceptance, before technical editing, formatting and proof reading. Using this free service, authors can make their results available to the community, in citable form, before we publish the edited article. We will replace this Accepted Manuscript with the edited and formatted Advance Article as soon as it is available.

You can find more information about Accepted Manuscripts in the [Information for Authors](#).

Please note that technical editing may introduce minor changes to the text and/or graphics, which may alter content. The journal's standard [Terms & Conditions](#) and the [Ethical guidelines](#) still apply. In no event shall the Royal Society of Chemistry be held responsible for any errors or omissions in this Accepted Manuscript or any consequences arising from the use of any information it contains.

COMMUNICATION

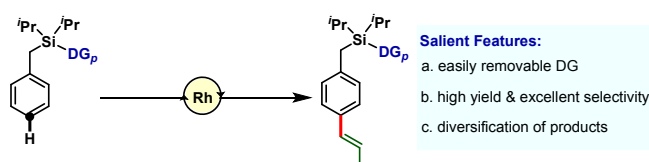
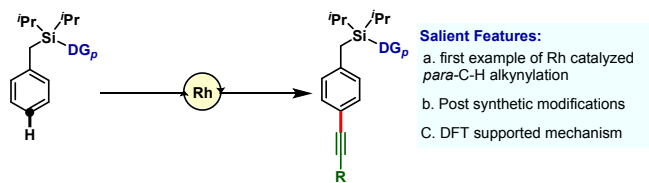
View Article Online
DOI: 10.1039/D3SC03528JDirecting Group Assisted *para*-Selective C–H Alkynylation of Unbiased Arenes Enabled by Rhodium CatalysisUttam Dutta,^{[a]#} Gaurav Prakash,^{[a]#} Kirti Devi,^[a] Kongkona Borah,^[a] Xinglong Zhang,^{*[b]} Debabrata Maiti^{*[a]}Received 00th January 20xx,
Accepted 00th January 20xx

DOI: 10.1039/x0xx00000x

ABSTRACT: Regioselective C–H alkynylation of arenes *via* C–H activation is challenging yet a highly desirable transformation. In this regard, directing group assisted C(sp²)–H alkynylation of arenes offers a unique opportunity to ensure precise regioselectivity. While the existing methods are majorly centered around *ortho*-C–H alkynylation and a few for *meta*-C–H alkynylation, the DG-assisted *para*-selective C–H alkynylation is yet to be reported. Herein we disclose the first report on Rh-catalyzed *para*-C–H alkynylation of sterically and electronically unbiased arenes. The *para*-selectivity is achieved with the assistance of a cyano-based directing template and the selectivity remained unaltered irrespective of the steric and electronic influence of the substituents. The post-synthetic modification of synthesized *para*-alkynylated arenes is also demonstrated. The mechanistic intricacies of the developed protocol are elucidated through experimental and computational studies.

Acetylene motifs are prevalent in various natural products, agrochemicals, pharmaceuticals, and in materials.¹ It not only provides a unique linear and rigid backbone in molecular arrangement but it also renders a platform to harness the benefit of extended π -conjugated system in organo-electronic materials.² The easily transformable nature of the alkyne is an additional advantage as it offers a unique opportunity to diversify the drug molecules and biologically active molecules *via* triple bond functionalization.³ Therefore, alkynylation of arenes is considered as one of the most desirable transformations. In this regard, palladium catalyzed Sonogashira coupling reaction is the most versatile and generalized method to synthesize aryl alkynes using aryl (pseudo)halides and terminal alkynes.⁴ However, utilization of prefunctionalized aryl

(pseudo)halides is the major drawback of this method and it inhibits wide application in synthetic chemistry.

a. Previous work: DG-assisted Rh-catalyzed *para*-C–H olefinationb. Present work: DG-assisted Rh-catalyzed *para*-C–H alkynylationScheme 1. Directing group assisted Rh catalyzed *para*-C–H functionalization of arenes

In search of alternative approaches that preclude the usage of prefunctionalized arenes, a number of methods were developed in which arene-C(sp²)–H alkynylation was achieved using terminal alkynes or activated alkynes, *e.g.* ethynylbenziodoxolone (EBX) reagents⁵ or haloalkynes.⁶ Notably, success of these methods require electronically activated arenes⁷ or arenes bearing a chelating directing group (DG).⁸ While the former strategy delivers an alkynylated product based on the electronic effect of its substituents, the later ensures the regioselective alkynylation of the targeted arene depending on the nature of the directing group. The applicability of electronically controlled C(sp²)–H alkynylation method is limited to a certain class of substrates bearing electron releasing functional groups. Contrary to that, DG-assisted C–H activation strategy offers a broad scope and practical method to ensure regioselective C–H alkynylation. However, the majority of the available methods are limited to *ortho*-C–H alkynylation, which proceed *via* a thermodynamically favourable five to six membered metallacyclic intermediate. Examples pertaining to the DG-assisted distal *meta*- or *para*-C–H alkynylation, which proceeded *via* a large

^a IIT Bombay, Department of Chemistry, Powai, Mumbai 400076, India.^b Institute of High Performance Computing (IHPC), Agency for Science, Technology and Research (A*STAR), Singapore, Singapore.

E-mail: zhang_xinglong@ihpc.a-star.edu.sg (X. Z.); dmaiti@iitb.ac.in (D.M.)

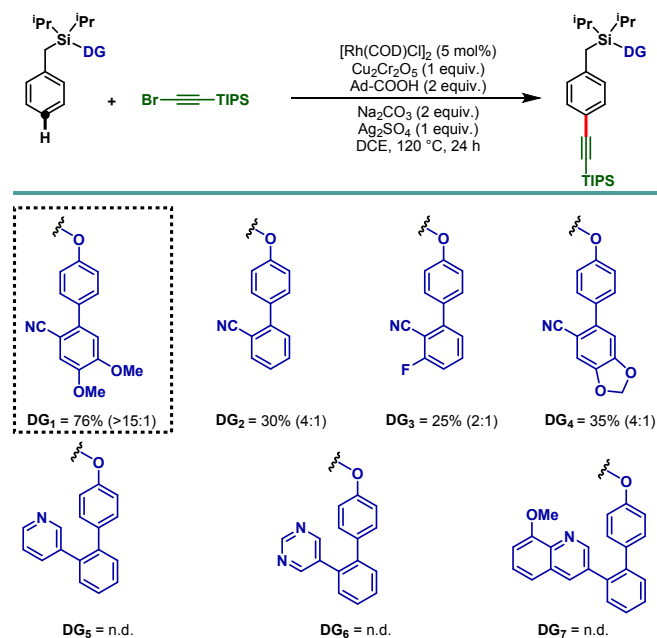
#These authors contributed equally.

Electronic Supplementary Information (ESI) available: See DOI: 10.1039/x0xx00000x



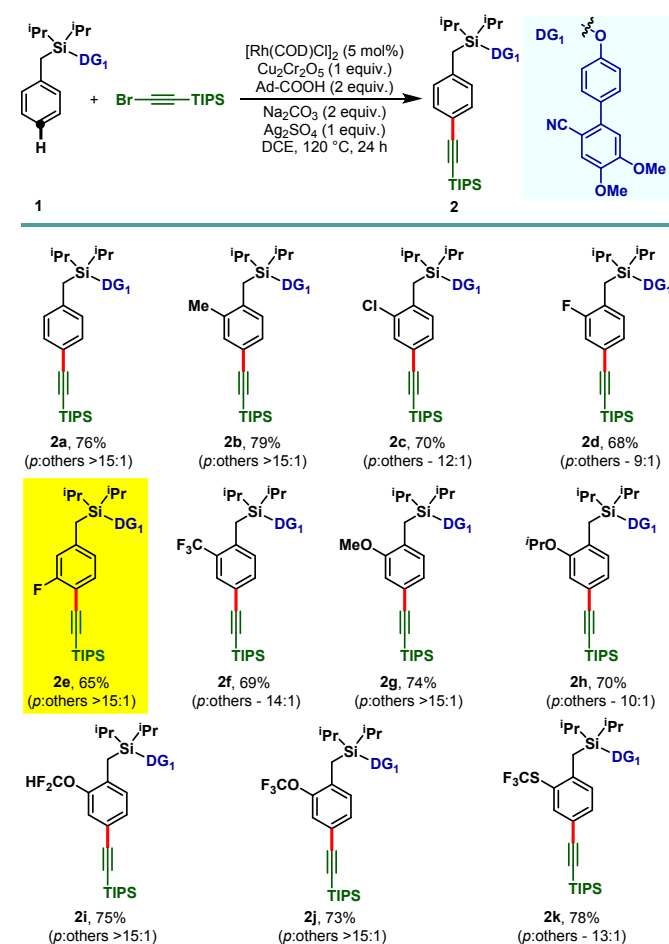
macrocyclic cyclophane-type intermediate,⁹ is scarce in the literature. However, the state-of-the-art methodologies that are available to perform *para*-selective C–H functionalization of arenes, are either relying on the electronic control of the arene or by the prudent design of the templates. In this regard, *para*-selective borylation was achieved by the group of Itami with the help of an elegantly designed bulky ligand.¹⁰ The group of Nakao reported the *para*-selective alkylation and borylation under nickel¹¹ and iridium¹² catalyzed condition, respectively, by exploiting the steric governance of Al-based Lewis acid. A specialized L-shaped template was developed by Chattopadhyay and co-workers to perform *para*-selective borylation of aromatic esters.¹³ *Para*-selective alkylation of aniline derivatives was demonstrated by Frost under Ru-catalyzed conditions in 2017.¹⁴ Subsequently, similar catalytic platform was used by Zhao to perform *para*-selective difluoromethylation of anilides¹⁵ and Ketoximes¹⁶. In 2020, they also reported *para*-selective difluoromethylation using Iron(tetraphenylporphyrinato) chloride [Fe(TPP)Cl].¹⁷ Evidently, these protocols are extremely limited to certain class of substrates as well as functionalizations. In order to establish a robust protocol to access selective distal C–H alkylation of sterically and electronically unbiased arenes, we rely on directing group assisted C–H activation technique. The group of Yu, in this regard, has demonstrated a *meta*-C–H alkylation protocol using an *ortho*-directing group under palladium-norbornene (Pd-NBE) cooperative catalysis.¹⁸ Our group has also developed the *meta*-selective alkylation protocols employing previously developed *meta*-directing group under both palladium^{19a} and rhodium^{19b} catalyzed conditions. However, the notable development in the realm of selective *para*-C–H alkylation is yet to be reported.

Table 1. Directing group (DG) optimization



A suitable directing group to ensure the selective *para*-C–H activation requires to maintain a precise geometric orientation between the desired C–H bond and the directing group, so that the

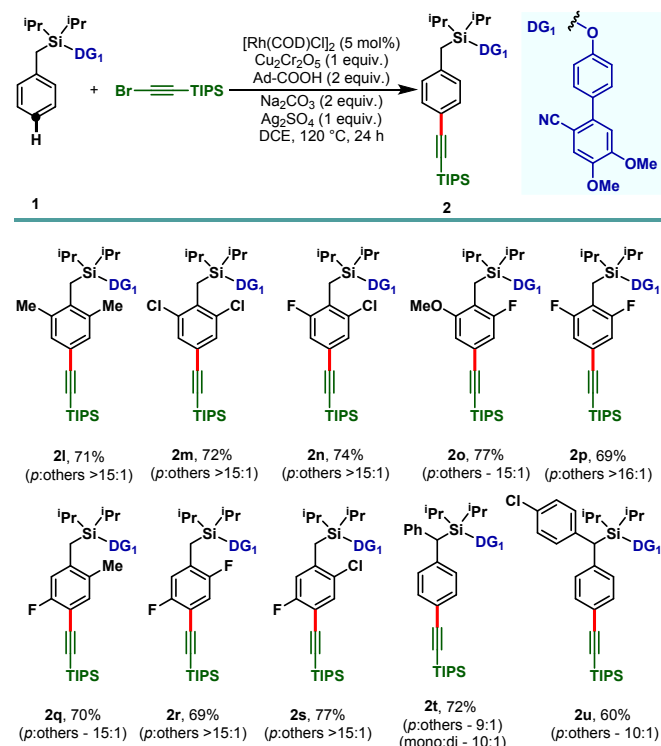
transition metal catalyst can be accommodated at the proximity of the desired *para*-C–H bond.^{20, 9c} In this regard, a D-shaped template was contemplated by our group in 2015 to execute the *para*-selective C–H functionalization.²⁰ With this D-shaped template, thus far, *para*-selective C–H olefination,^{20, 21a} acetoxylation,^{20, 21b} silylation,^{21c} ketonization,^{21d} cyanation,^{21e} and arylation^{21f} was achieved. In 2021, Li and coworkers developed a novel pyridine-based *para*-directing template to harness *para* selective olefination under Pd-catalyzed conditions.²² Despite the seminal progress in this realm, the widespread application of the template assisted *para*-selective C–H activation is yet to be achieved. We, therefore, became interested in harnessing *para*-selective C–H alkylation of arenes by employing the D-shaped template. Nevertheless, *para*-selective alkylation of aniline derivatives was achieved by Waser^{7c} and Fernández-Ibáñez^{7d} using Au and Pd catalyst, respectively. These methods were found to be effective with electron rich aniline derivatives. van Gemmeren and co-workers also reported sterically controlled C–H alkylation of arenes under Pd-catalyzed conditions at the distal *meta*-position.²³



Scheme 2. Rh-catalyzed *para*-C–H alkylation of mono-substituted arenes.

Our investigation in *para*-selective C–H functionalization relying on template assistance is majorly centered around the palladium catalyzed conditions in combination with super stoichiometric silver

oxidant.^{20, 21} In sharp contrast, broader catalytic potential of other transition metals is yet to be explored. To the best of our knowledge, *para*-selective C–H olefination is the only instance, reported till date under Rh-catalyzed conditions (Scheme 1a).²⁴ As our concerted focus is devoted in diversifying the template assisted regioselective distal C–H functionalization method, herein we disclosed the first example of DG-assisted *para*-C–H alkynylation of arenes *via* inverse Sonogashira coupling reaction utilizing Rh-catalyst (Scheme 1b). More importantly, the desired transformation is unattainable under Pd-catalyzed conditions. Therefore, the present method provides a complementary platform to Pd-catalysis in achieving selective distal C–H functionalization of arenes.

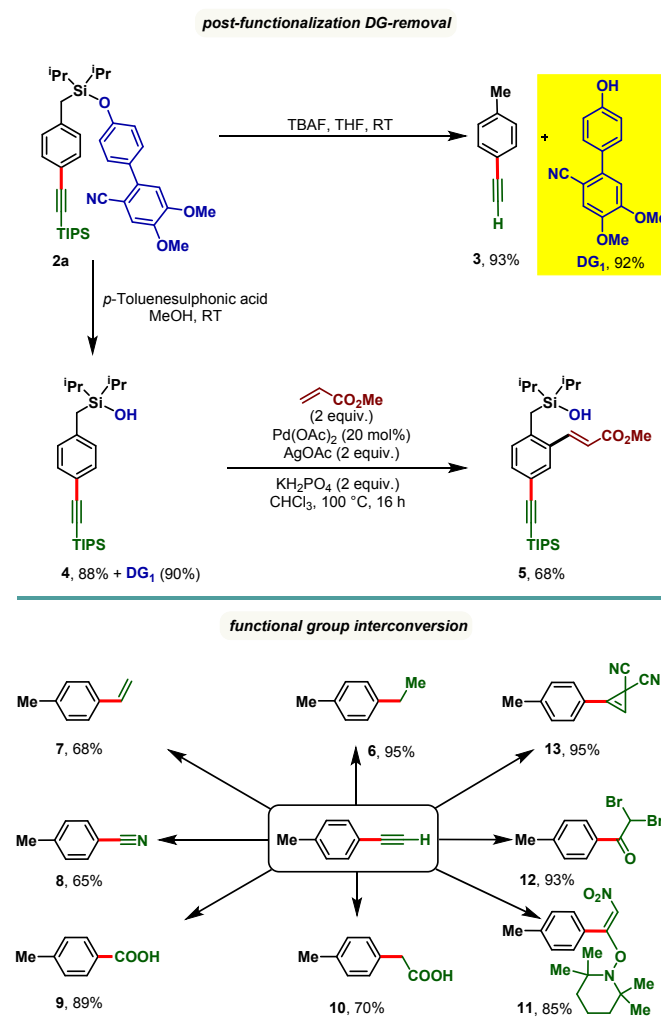


Scheme 3. Rh-catalyzed *para*-C–H alkynylation of di-substituted arenes.

To demonstrate the feasibility of *para*-selective C–H alkynylation reaction, we chose model toluene scaffold, equipped with the electron rich, dimethoxy substituted cyano-based D-shaped template (**DG₁**) and (bromoethynyl)triisopropylsilane as alkynylating coupling partner. Initial attempt of *para*-C–H alkynylation using [RhCp*Cl₂]₂ as catalyst, CuCl₂ as oxidant and Ag₂CO₃ as co-oxidant in the presence of trifluoroacetic acid (TFA) in dichloroethane (DCE) solvent gave the desired product in 20% yield. While optimizing the Rh-catalysts, slight improvement in yield was observed with the [Rh(cod)Cl]₂. Rh₂(OAc)₄ or Rh(PPh₃)₃Cl were found to be ineffective. Further optimization of the reaction parameters revealed that the combination of dual additives consisting of Cu₂Cr₂O₅ and Ag₂SO₄ furnished the desired compound in 51% yield. Finally, synthetically useful yield (76% isolated) and selectivity (*para:others* >15:1) was achieved when a combination of 1-adamantanecarboxylic acid and Na₂CO₃ were used as an acid and base additive, respectively. We also tried using oxygen as green oxidant along with catalytic amount of

$\text{Cu}_2\text{Cr}_2\text{O}_5$ but the reaction outcome was not good compared to $\text{Cu}_2\text{Cr}_2\text{O}_5$ as the stoichiometric oxidant.²⁵ Notably, electronically modified cyano-based weakly coordinating directing groups (DG_2 , DG_3 , and DG_4) were also examined and all of them were found to be less efficient in comparison to DG_1 (Table 1). Additionally, relatively strongly coordinating pyridine (DG_5), pyrimidine (DG_6) and quinoline (DG_7) based directing groups failed to produce the alkynylated compounds under the developed reaction conditions.

With the optimized reaction conditions, the mono substituted toluene-based scaffolds tethered with DG₁ was examined to demonstrate the generality of the developed method (Scheme 2). Both the electron donating as well as electron withdrawing substituents delivered the desired *para*-alkynylated compounds with excellent yield and acceptable selectivity.



Scheme 4. Directing group (DG) removal and post-synthetic modification of *para*-alkynylated arenes.

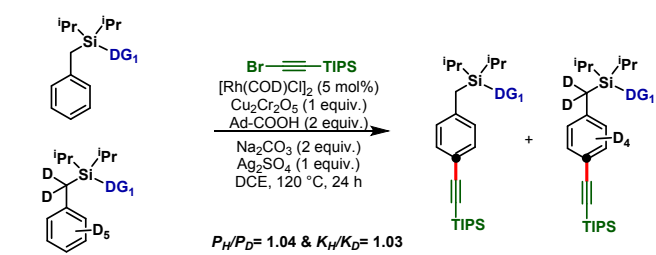
Electron releasing methyl substituent provided the desired product (**2b**) in 79% yield with greater than 15:1 selectivity, the electron deficient haloarenes (**2c-2e**) and *ortho*-trifluoromethyl arene also gave the *para*-alkynylated compounds (**2f**) in good yield and selectivity. Additionally, arenes bearing ethers (**1g – 1j**) and thioether (**1k**) were tolerated under the reaction conditions and the desired

products were obtained without compromising the yield and selectivity. The versatility of the developed protocol was further demonstrated with disubstituted arenes. *para*-C–H alkynylation with both the 2,6- (**1l** – **1p**) and 2,5-disubstituted arenes (**1q** – **1s**) proceeded smoothly and the desired products were obtained in synthetically useful yield and selectivity (Scheme 3). Notably, while the *meta*-F substrate provided the *para*-alkynylated compound in 65% yield with >15:1 selectivity, relatively bulky *meta*-substituents such *meta*-CH₃, *meta*-Cl, and *meta*-CF₃ scaffolds delivered majorly the *meta*-alkynylated compounds. We reasoned that the bulkiness of these substituents prevents the accessibility of the *para*-C–H bond and therefore the sterically less hindered *meta*-C–H bond was activated. Further, the applicability of the protocol was extended to α -substituted toluene derivatives (**1t** and **1u**). Notably, the α -phenyl toluene derivative majorly afforded the mono-alkynylated product (**2t**, mono:di - 10:1). It is evident from the scope of the reaction that the electronic nature of the arenes and steric influence of the substituents did not alter the reaction outcome in terms of yield and *para*-selectivity. Thus, the protocol offers an opportunity to expand the scope of regioselective distal *para*-C–H alkynylation to accommodate a wide range of steric and electronic demands of substrates. However, the developed protocol failed to accommodate other alkyne coupling partners such as 1-bromo-2-phenylacetylene, 1-bromohept-1-yne, ethyl 3-bromopropiolate and (bromoethynyl)trimethylsilane. The phenomenon could be justified by the coordinating propensity of π bonds to the Rh center, which was also highlighted in the previous literature reports.²⁶

The synthetic utility of the developed *para*-selective C–H alkynylation protocol was further demonstrated through the removal of appended directing group as well as through functional group interconversion (Scheme 4). Treatment of **2a** with tetrabutylammonium fluoride (TBAF) furnished *p*-tolylacetylene (**3**) along with directing group (DG₁) in quantitative yield. It is worth noting that the 4'-hydroxy-4,5-dimethoxy-[1,1'-biphenyl]-2-carbonitrile (DG₁)

could be attached further to prepare our starting materials, highlighting the reusability of the directing group. Compound **2a** treated with *p*-toluenesulfonic acid in methanol resulted a silanol derivative, **4**. Taking the advantage of *ortho*-directing capability of silanol motif, **4** was subjected to Pd catalyzed *ortho*-C–H olefination reaction conditions and an *ortho*-olefinated and *para*-alkynylated compound, **5** was obtained in 68% yield. Considering the easy transformability of alkynes, the alkynylated product (**3**) was reduced to corresponding alkane (**6**) and alkene (**7**), and oxidized to benzonitrile (**8**), benzoic acid (**9**), and phenyl acetic acid (**10**) derivative. Additionally, oxynitration (**11**), oxydibromination (**12**), and cyclopropanation (**13**) reactions were achieved with good to excellent yields.

Isotope labeling experiments were performed involving an intermolecular competition using substrate and its deuterated analogue d7 and a P_H/P_D value of 1.04 and k_H/k_D value of 1.03 were obtained. This implies that the C–H activation step is not the overall rate-limiting step of this reaction. Further, order determination studies with respect to the substrate revealed that the reaction was first order with respect with substrate and first order with respect to alkyne coupling partner, indicating that both the substrate and the alkyne coupling partner are involved in the rate-limiting step.



Scheme 5. Kinetic isotopic experiments with deuterium-labeled substrate.



COMMUNICATION

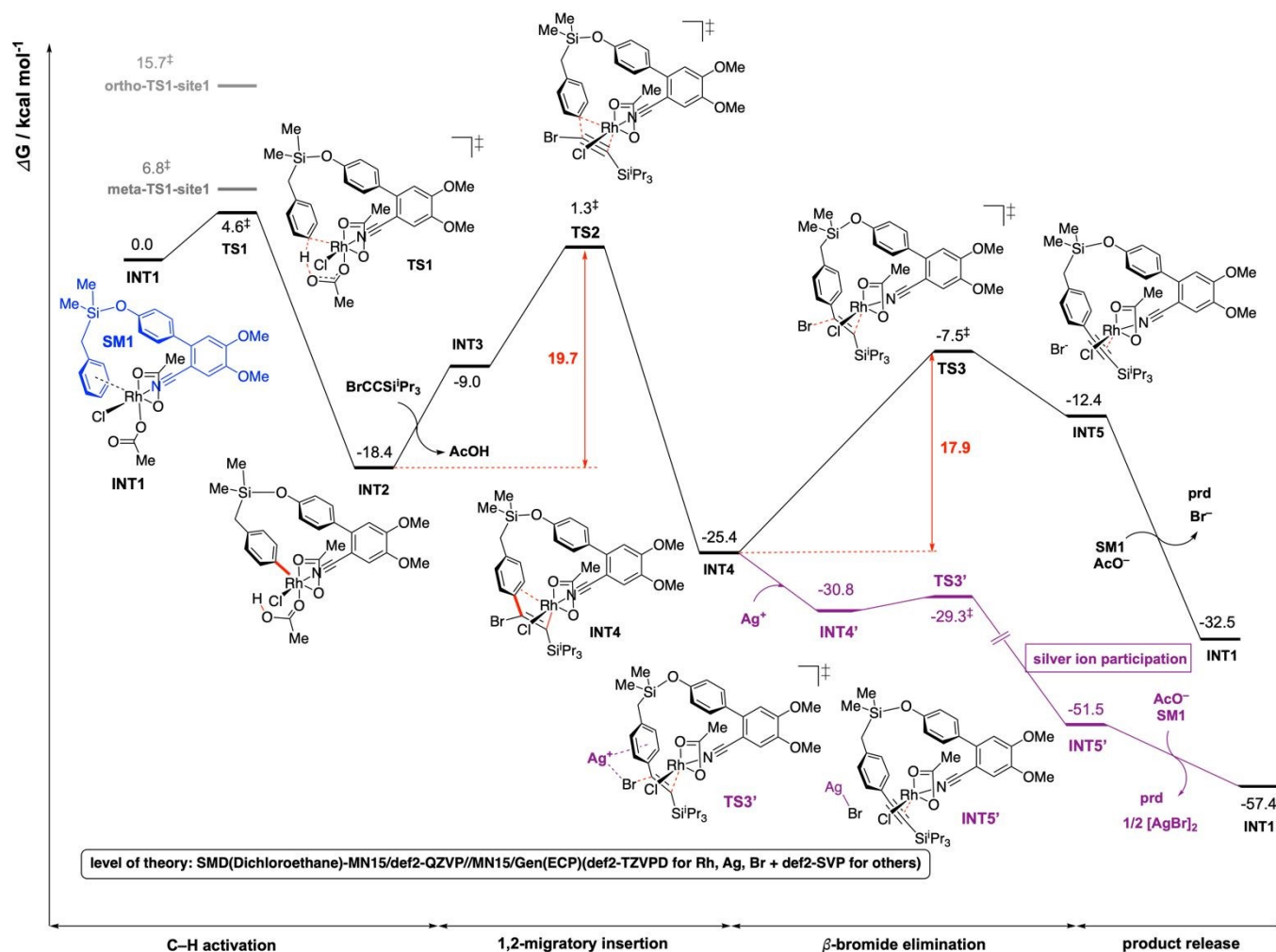
View Article Online
DOI: 10.1039/D3SC03528J

Figure 1. Gibbs energy profile for the Rh-catalyzed C(sp^2)-H alkynylation of arenes. DFT optimized key transition structures are shown in Figure 2.

Computational studies: For computational investigation of the mechanism of present Rh-catalyzed *para*-selective C(sp^2)-H alkynylation of arenes, density functional theory (DFT) was employed. Simplified arene, **SM1**, where the isopropyl groups on the Si atom were replaced by methyl groups, and bromoethynyltriisopropylsilane (hereafter bromoalkyne) were used for modelling. The use of i Pr groups on Si benefits from favorable Thorpe-Ingold effect making the formation of rhodacycle easier than Me groups, but this simplification should not affect the reaction mechanism – any favorable barriers calculated with this simplified model are expected to be favorable for the i Pr analogue. The adamantane-1-carboxylate is simplified to acetate in the DFT

calculations to save computational cost. The adamantyl group provides sterics to the molecules and in computational modelling we avoid conformations that would give rise to clashes if adamantane-1-carboxylate was used instead of acetate. We expect that the carboxylate group of the simplified acetate to provide similar metal-ligand interactions with Rh center as the adamantane-1-carboxylate. Gibbs energy profiles were computed at SMD (dichloroethane)-MN15²⁷/def2-QZVP//MN15/GENECP (def2-TZVPD for Br,²⁸ Rh²⁹ and Ag²⁹ + def2-SVP^{30, 31} for others) level of theory where a mixed basis set was used for geometry optimization (See SI section 6 for full details).³²

TS1 (<i>para</i>)	<i>meta</i> -TS1-site1	<i>ortho</i> -TS1-site1
$\Delta G^\ddagger = 4.6 \text{ kcal mol}^{-1}$	$\Delta G^\ddagger = 6.8 \text{ kcal mol}^{-1}$	$\Delta G^\ddagger = 15.7 \text{ kcal mol}^{-1}$



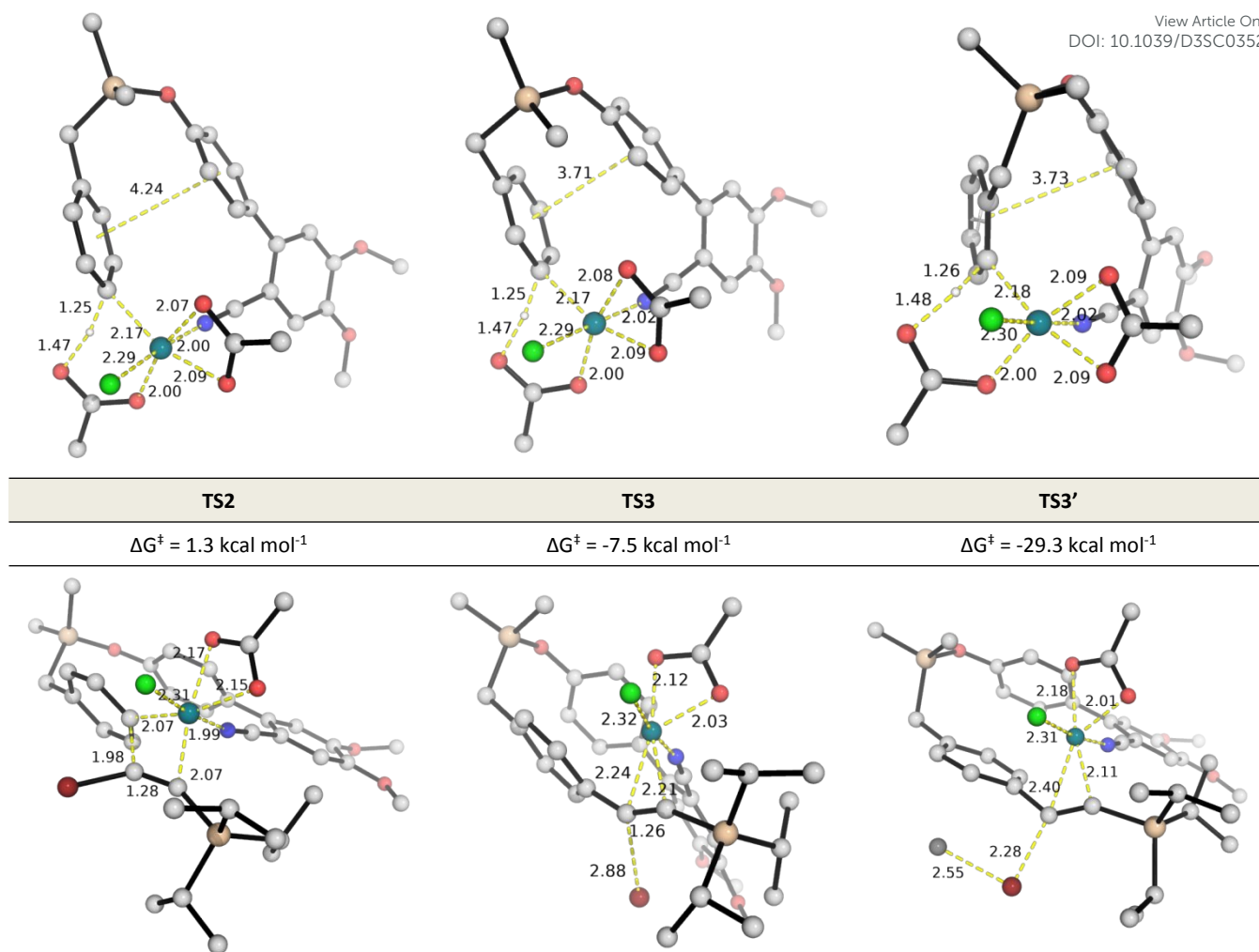


Figure 2. DFT optimized TS structures for the C–H activation at different arene sites (**TS1s**), migratory insertion (**TS2**) and β -bromide elimination without (**TS3**) and with (**TS3'**) silver ion participation. All Gibbs energies are taken with **INT1** as zero reference. See Figure S5 for C–H activation TSs of all possible sites.

The overall Gibbs free energy profile is shown in Figure 1. First, the $\text{Cu}_2\text{Cr}_2\text{O}_5$ additive may play a role in oxidising the Rh(I) precatalyst to Rh(III) which actively participates in the catalytic cycle. Computed C–H activation barriers indicate a kinetic preference for the activation of the *para*-C–H bond (see SI, section 6.3) by a factor of 16:1 over the *meta* position and ~ 1.5 million:1 over the *ortho* position. Detailed investigation of the steric and electronic influences of these TSs suggests that ring strains in the *meta*-C–H activation transition structures (*meta*-**TS1-site1** and *meta*-**TS1-site2**, Figure S5) are the lowest (Table S9) while *para*-activation has the most favorable orbital overlap between the d-orbital on Rh-metal and the π -orbital on the arene (Figure S6). Taken together, the activation of the *para*-C–H bond (**TS1**) is lower than the activation of the *meta*-C–H bond (by 2.2 kcal mol $^{-1}$ for *meta*-**TS1-site1** and by 3.9 kcal mol $^{-1}$ for *meta*-**TS1-site2**) and the activation of the *ortho*-C–H bond (by 11.1 kcal mol $^{-1}$ for *ortho*-**TS1-site1** and by 13.9 kcal mol $^{-1}$ for *ortho*-**TS1-site2**). Additionally, the C–H activation step was found not to be the turnover frequency-determining transition state (TDTS) of the reaction as the formation of the rhodacycle after C–H activation is

highly exergonic and irreversible, with the subsequent barrier for 1,2-migratory insertion (19.7 kcal mol $^{-1}$ from the C–H activated complex **INT2** to **TS2**) lower than the barrier from **INT2** back to **INT1** (23.0 kcal mol $^{-1}$ via **TS1**). In the absence of silver ion participation, the β -bromide elimination step (**TS3**) has a barrier of 17.9 kcal mol $^{-1}$. In the presence of silver ions, however, the β -bromide elimination step has a much lower barrier (**TS3'**, barrier of 1.5 kcal mol $^{-1}$), this is potentially favored by the exergonic formation of AgBr salt.^{19a} In either case, the 1,2-migratory insertion of bromoalkyne, **TS2**, will be the overall TDTS and the C–H activated rhodacycle, **INT2**, will be the TDI. Since the bromoalkyne enters after the TDI and participates in the TDTS, this predicts a first order dependence of the reaction rate on the concentration of the bromoalkyne substrate. In addition, as the C–H activated substrate also participates in the TDTS, a first order dependence on the substrate is similarly expected from the computed energy profile. Both of these predictions are consistent with our experimental order determination measurements (first order with respect to substrate and bromoalkyne). Finally, the alkyne product dissociates from the catalyst-product complex



INT5', which releases the product and enters the next catalytic cycle by regenerating **INT1**. Combined experimental and computational mechanistic investigations suggest that the present Rh-catalyzed $C(sp^2)$ -H alkynylation proceeds via non-rate-determining, irreversible regioselective C-H activation at the *para*-position, followed by turnover-frequency determining 1,2-migratory insertion of bromoalkyne substrate. This is then followed by the β -bromide elimination step which can be greatly facilitated in the presence of silver ion participation. Our computed energy profile is in agreement with experimental kinetic isotope effects showing that C-H activation is not rate-determining and the measured rate law with first order dependence on both the substrate and the alkyne coupling partner.

Conclusions

In summary, we have developed an unprecedented route for reusable template-assisted Rh catalyzed *para*-C-H alkynylation. The protocol was well tolerated with different kinds of substituents on the arene ring. Further late-stage modification of the product and functional group inter-conversion were performed. The mechanistic studies were supported by computational studies proving that although regio-determining, the C-H activation is not the overall rate limiting step. Instead, migratory insertion of the alkyne coupling partner is overall rate-determining. We anticipate that this methodology will greatly broaden the scope of functionalization in the realm of remote *para*-C-H activation.

Author Contributions

U. D., G. P. and D. M. conceived the project. U. D., G. P., K. D. and K. B. completed the experimental work. X. Z. designed and performed the computational studies and analysed the results. X. Z. and D. M. wrote the manuscript and supervised the work. All authors contributed in writing the manuscript.

Conflicts of interest

The authors declare no conflict of interest.

Acknowledgements

This activity is funded by SERB-India (TTR/2021/000108). Financial support received as fellowship from CSIR-India (to G. P.) is gratefully acknowledged. X.Z. acknowledges the support from the Agency for Science, Technology and Research (A*STAR) under its Career Development Fund (CDF Project Number C210812008) and Manufacturing, Trade and Connectivity (MTC) Young Individual Research Grants (YIRG grant number M22K3c0091) for this work. X.Z. acknowledges the partial use of supercomputers in the National Supercomputing Centre (NSCC), Singapore (<https://www.nsc.sg>) and the A*STAR Computational Resource Center (A*CRC) for computations performed in this work.

Notes and references

View Article Online

DOI: 10.1039/D3SC03528J

1. a) F. Diederich, P. J. Stang, R. R. Tykwinski, Eds.; Wiley-VCH: Weinheim, Germany, 2005. (b) G. V. Boyd, S. Patai, Ed.; Wiley: Hoboken, NJ, 1994; Chapter 5. c) H. C. Kolb, M. G. Finn, K. B. Sharpless, *Angew. Chem. Int. Ed.*, 2001, **40**, 2004-2021; d) A. Fürstner and P. W. Davies, *Chem. Commun.*, 2005, 2307.; e) A. Fürstner, *Chem. Soc. Rev.*, 2009, **38**, 3208-3221; f) M. G. Finn and V. V. Fokin, *Chem. Soc. Rev.*, 2010, **39**, 1231; g) J. P. Brand and J. Waser, *Chem. Soc. Rev.*, 2012, **41**, 4165-4179; h) C. Obradors and A. M. Echavarren, *Acc. Chem. Res.*, **2014**, **47**, 902-912; i) L. Fensterbank and M. Malacria, *Acc. Chem. Res.*, 2014, **47**, 953-965; j) R. Dorel and A. M. Echavarren, *Chem. Rev.*, 2015, **115**, 9028-9072; k) D. Hashmi and A. S. K. Hashmi, *Chem. Soc. Rev.*, 2016, **45**, 1331-1367; l) R. Talpur, K. Cox and M. Duvic, Efficacy and safety of topical tazarotene: a review. *Expert Opin. Drug Metab. Toxicol.* 2009, **5**, 195; m) Z.-Y. Yang, J.-Q. Yuan, M.-Y. Di, D.-Y. Zheng, J.-Z. Chen, H. Ding, X.-Y. Wu, Y.-F. Huang, C. Mao and J.-L. Tang, Gemcitabine Plus Erlotinib for Advanced Pancreatic Cancer: A Systematic Review with Meta-Analysis. *PLOS ONE* 2013, **8**, No. e57528.
2. a) T. M. Swager, Semiconducting Poly(arylene ethylene)s. In *Acetylene Chemistry: Chemistry, Biology and Material Science*; F. Diederich, P. J. Stang, R. R. Tykwinski, Eds.; Wiley-VCH: Weinheim, 2005. b) F. Diederich and Y. Rubin, *Angew. Chem., Int. Ed.*, 1992, **31**, 1101. c) U. H. F. Bunz, Y. Rubin and Y. Tobe, *Chem. Soc. Rev.*, 1999, **28**, 107.
3. (a) L. Hintermann and A. Labonne, *Synthesis*, 2007, **8**, 1121-1150; (b) R. Severin and S. Doye, *Chem. Soc. Rev.*, 2007, **36**, 1407-1420; (c) R. Chinchilla and C. Najera, *Chem. Rev.*, 2014, **114**, 1783-1826; d) J.-F. Lutz, *Angew. Chem. Int. Ed.*, 2007, **46**, 1018-1025; e) M. Meldal and C. W. Tornøe, *Chem. Rev.*, 2008, **108**, 2952-3015; f) A. Fürstner, *Handbook of Metathesis*; Wiley-VCH Verlag GmbH & Co. KGaA: 2015; p 445. g) J. Li and D. Lee, *Handbook of Metathesis*; Wiley-VCH Verlag GmbH & Co. KGaA: 2015; p 381.
4. Selected examples of Sonogashira coupling reaction: a) K. Sonogashira, *J. Organomet. Chem.*, 2002, **653**, 46-49; b) E. Negishi and L. Anastasia, *Chem. Rev.*, 2003, **103**, 1979-2018; c) A. O. King and N. Yasuda, *Top. Organomet. Chem.*, 2004, **6**, 205-245; d) H. Doucet and J.-C. Hierso, *Angew. Chem., Int. Ed.*, 2007, **46**, 834-871; e) H. Plenio, *Angew. Chem., Int. Ed.*, 2008, **47**, 6954-6956; f) R. Chinchilla and C. Najera, *Chem. Soc. Rev.*, 2011, **40**, 5084-5121; g) R. Chinchilla and C. Nájera, *Chem. Rev.*, 2014, **114**, 1783-1826; h) D. Wang and S. Gao, *Org. Chem. Front.*, 2014, **1**, 556-566.
5. For selected reviews on use of EBX see: a) V. V. Zhdankin and P. J. Stang, *Tetrahedron*, 1998, **54**, 10927-10966; b) V. V. Zhdankin and P. J. Stang, *Chem. Rev.*, 2008, **108**, 5299-5358.
6. For use of Haloalkynes see: (a) A. S. Dudnik and V. Gevorgyan, *Angew. Chem., Int. Ed.* 2010, **49**, 2096-2098; (b) Y. Ano, M. Tobisu and N. Chatani, *J. Am. Chem. Soc.*, 2011, **133**, 12984-12986; (c) Y. Ano, M. Tobisu and N. Chatani, *Synlett*, 2012, **23**, 2763-2767; (d) J. He, M. Wasa, K. S. L., Chan and J.-Q. Yu, *J. Am. Chem. Soc.*, 2013, **135**, 3387-3390; e) K. Kobayashi, M. Arisawa and M. Yamaguchi, *J. Am. Chem. Soc.*, 2002, **124**, 8528-8529; f) I. V. Seregin, V. Ryabova and V. Gevorgyan, *J. Am. Chem. Soc.*, 2007, **129**, 7742-7743;
7. Electronic controlled alkynylation: a) T. de Haro and C. Nevado, *J. Am. Chem. Soc.*, 2010, **132**, 1512-1513; b) Y. Wei, H. Zhao, J. Kan, W. Su and M. Hong, *J. Am. Chem. Soc.*, 2010, **132**, 2522-2523; c) J. P. Brand and J. Waser, *Org. Lett.*, 2012, **14**, 744-747; d) K.-Z. Deng, W.-L. Jia and M. A. Fernández-Ibáñez, *Chem. Eur. J.*, 2021, e202104107.
8. Selected examples on DG-assisted $C(sp^2)$ -H alkynylation with alkynyl halide: a) M. Tobisu, Y. Ano and N. Chatani, *Org. Lett.*, 2009, **11**, 3250-3252; b) Y. Ano, M. Tobisu and N. Chatani, *Org. Lett.*, 2012,



- 14**, 354–357; c) M. Shang, H.-L. Wang, S.-Z. Sun, H.-X. Dai and J.-Q. Yu, *J. Am. Chem. Soc.*, 2014, **136**, 11590–11593; d) F. Xie, Z. Qi, S. Yu and X. Li, *J. Am. Chem. Soc.*, 2014, **136**, 4780–4787; e) H. M.-F. Viart, A. Bachmann, W. Kayitare and R. Sarpong, *J. Am. Chem. Soc.*, 2017, **139**, 1325–1329; f) C. Feng and T.-P. Loh, *Angew. Chem., Int. Ed.*, 2014, **53**, 2722–2726; *Angew. Chem.*, 2014, **126**, 2760–2764; g) Y.-H. Liu, Y.-J. Liu, S.-Y. Yan and B.-F. Shi, *Chem. Commun.*, 2015, **51**, 11650–11653; h) N. Sauermann, M. J. Gonzalez and L. Ackermann, *Org. Lett.*, 2015, **17**, 5316–5319; i) Z.-Z. Zhang, B. Liu, C.-Y. Wang and B.-F. Shi, *Org. Lett.*, 2015, **17**, 4094–4097; j) Y.-J. Liu, Y.-H. Liu, X.-S. Yin, W.-J. Gu and B.-F. Shi, *Chem. Eur. J.*, 2015, **21**, 205–209; k) P. Wang, G.-C. Li, P. Jain, M. E. Farmer, J. He, P.-X. Shen and J.-Q. Yu, *J. Am. Chem. Soc.*, 2016, **138**, 14092–14099; l) R. Boobalan, P. Gandeepan and C.-H. Chieng, *Org. Lett.*, 2016, **18**, 3314–3317; m) V. G. Landge, G. Jaiswal and E. Balaraman, *Org. Lett.*, 2016, **18**, 812–815; n) Z. Ruan, S. Lackner and L. Ackermann, *ACS Catal.*, 2016, **6**, 4690–4693; o) Z. Ruan, N. Sauermann, E. Manoni and L. Ackermann, *Angew. Chem., Int. Ed.*, 2017, **56**, 3172–3176; p) E. Tan, O. Quinonero, M. Elena de Orbe and A. M. Echavarren, *ACS Catal.*, 2018, **8**, 2166–2172, and the references therein.
9. a) A. Dey, S. K. Sinha, T. K. Achar and D. Maiti, *Angew. Chem., Int. Ed.*, 2019, **58**, 10820–10843; b) S. Sasmal, U. Dutta, G. K. Lahiri and D. Maiti, *Chem. Lett.*, 2020, **49**, 1406–1420; c) G. Meng, N. Y. S. Lam, E. L. Lucas, T. G. Saint-Denis, P. Verma, N. Chekshin and J.-Q. Yu, *J. Am. Chem. Soc.*, 2020, **142**, 10571–10591; d) U. Dutta, S. Maiti, T. Bhattacharya and D. Maiti, *Science*, 2021, **372**, eabd5992; e) W. Ali and G. Prakash, *Chem. Sci.*, 2021, **12**, 2735–2759. f) J. Grover, G. Prakash, N. Goswami and D. Maiti, *Nature Communications*, 2022, **13**, 1085.
10. Y. Saito, Y. Segawa and K. Itami, *J. Am. Chem. Soc.*, 2015, **137**, 5193–5198.
11. a) S. Okumura, S. Tang, T. Saito, K. Semba, S. Sakaki and Y. Nakao, *J. Am. Chem. Soc.*, 2016, **138**, 14699–14704; b) S. Okumura and Y. Nakao, *Org. Lett.*, 2017, **19**, 584–587.
12. L. Yang, K. Semba and Y. Nakao, *Angew. Chem., Int. Ed.*, 2017, **56**, 4853–4857; *Angew. Chem.*, 2017, **129**, 4931–4935.
13. M. E. Hoque, R. Bisht, C. Haldar and B. Chattopadhyay, *J. Am. Chem. Soc.*, 2017, **139**, 7745–7748.
14. J. A. Leitch, C. L. McMullin, A. J. Paterson, M. F. Mahon, Y. Bhonoah and C. G. Frost, *Angew. Chem., Int. Ed.*, 2017, **56**, 15131–15135; *Angew. Chem.*, 2017, **129**, 15327–1533.
15. C. Yuan, L. Zhu, C. Chen, X. Chen, Y. Yang, Y. Lan and Y. Zhao, *Nat. Commun.*, 2018, **9**, 1189–1198.
16. C. Yuan, L. Zhu, R. Zeng, Y. Lan and Y. Zhao, *Angew. Chem., Int. Ed.*, 2018, **57**, 1277–1281; *Angew. Chem.*, 2018, **130**, 1291–1295.
17. W.-T. Fan, Y. Li, D. Wang, S.-J. Ji and Y. Zhao, *J. Am. Chem. Soc.*, 2020, **142**, 20524–20530.
18. P. Wang, G.-C. Li, P. Jain, M. E. Farmer, J. He, P.-X. Shen and J.-Q. Yu, *J. Am. Chem. Soc.*, 2016, **138**, 14092–14099.
19. a) S. Porey, X. Zhang, S. Bhowmick, V. Singh, S. Guin, R. S. Paton and D. Maiti, *J. Am. Chem. Soc.*, 2020, **142**, 3762–3774; b) S. Sasmal, G. Prakash, U. Dutta, R. Laskar, G. K. Lahiri and D. Maiti, *Chem. Sci.*, 2022, **13**, 5616–5621.
20. S. Bag, T. Patra, A. Modak, A. Deb, S. Maity, U. Dutta, A. Dey, R. Kancherla, A. Maji, A. Hazra, M. Bera and D. Maiti, *J. Am. Chem. Soc.*, 2015, **137**, 11888–11891.
21. a) T. Patra, S. Bag, R. Kancherla, A. Mondal, A. Dey, S. Pimparkar, S. Agasti, A. Modak and D. Maiti, *Angew. Chem., Int. Ed.*, 2016, **55**, 7751–7755; b) M. Li, M. Shang, H. Xu, X. Wang, H.-X. Dai and J.-Q. Yu, *Org. Lett.*, 2019, **21**, 540–544; c) A. Maji, S. Guin, S. Feng, A. Dahiya, V. K. Singh, P. Liu and D. Maiti, *Angew. Chem., Int. Ed.*, 2017, **56**, 14903–14907; (d) A. Maji, A. Dahiya, G. Lu, T. Bhattacharya, M. Brochetta, G. Zanoni, P. Liu and D. Maiti, *Nat. Commun.*, 2018, **9**, 3582; e) S. Pimparkar, T. Bhattacharya, A. Maji, A. Saha, R. Jayarajan, U. Dutta, G. Lu, D.W. Lupton and D. Maiti, *Chem. Eur. J.*, 2020, **26**, 11558; f) S. Maiti, Y. Li, S. Sasmal, S. Guin, T. Bhattacharya, G. K. Lahiri, R. S. Paton and D. Maiti, *Nat. Commun.*, 2022, **13**, 3963.
22. X. Chen, S. Fan, M. Zhang, Y. Gao, S. Lia and G. Li, *Chem. Sci.*, 2021, **12**, 4126.
23. A. Mondal, H. Chen, L. Flamig, P. Wedi and M. van Gemmeren, *J. Am. Chem. Soc.*, 2019, **141**, 18662–18667.
24. U. Dutta, S. Maiti, S. Pimparkar, S. Maiti, L. R. Gahan, E. H. Krenske, D.W. Lupton and D. Maiti, *Chem. Sci.*, 2019, **10**, 7426–7432.
25. S. Li, L. Cai, H. Ji, L. Yang, and G. Li, *Nature Communications*, 2016, **7**, 10443–10450.
26. J. He, M. Wasa, K. S. L. Chan and J.-Q. Yu, *J. Am. Chem. Soc.* **2013**, **135**, 3387–3390.
27. H. S. Yu, X. He, S. L. Li and D. G. Truhlar, *Chem. Sci.*, 2016, **7**, 5032–5051.
28. D. Rappoport and F. Furche, *J. Chem. Phys.*, 2010, **133**, 134105–134116.
29. D. Andrae, U. Häußermann, M. Dolg, H. Stoll and H. Preuß, *Theor. Chim. Acta.*, 1990, **77**, 123–141.
30. F. Weigend and R. Ahlrichs, *Phys. Chem. Chem. Phys.*, 2005, **7**, 3297–3305.
31. F. Weigend, *Phys. Chem. Chem. Phys.*, 2006, **8**, 1057–1065.
32. M. J. Frisch, G. W. Trucks, H. B. Schlegel, G. E. Scuseria, M. A. Robb, J. R. Cheeseman, G. Scalmani, V. Barone, G. A. Petersson, H. Nakatsuji, et al. Gaussian 16, Revision B.01. 2016.

